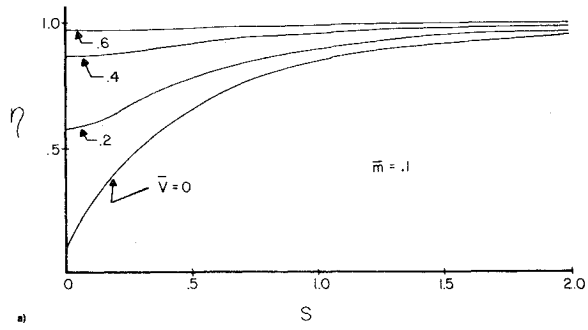

Fig. 3a Variation of transfer efficiency with speed ratio.

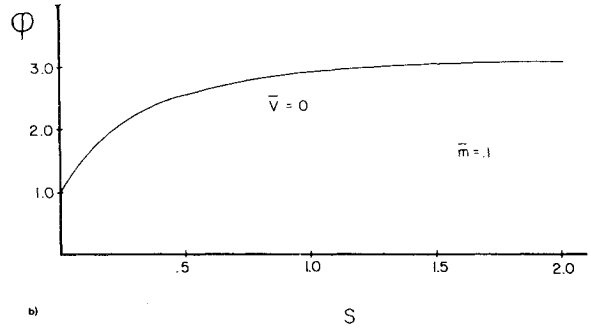

Fig. 3b Variation of thrust (momentum) augmentation with speed ratio.

insufficient energy to overcome the pressure gradient in the diffuser.

Since the momentum at position 3 is greater than that at 0, there must be a net force to the left on the earth supporting the track arrangement. This is analogous to the force transmitted to the ejector shroud by the internal pressure distribution which becomes the usable force on the aircraft.

The relative effect of inlet area ratio may be seen in the mass ratio $\bar{m}$. A small $\bar{m}$ corresponds to a high inlet area ratio and leads (in the ideal, no-loss case) to improved performance. The analogy to the primary nozzle thrust efficiency is the ratio of the actual velocity of mass M_0 at position 1 to its velocity at that position with no friction losses. The difference between these velocities is analogous to the flow losses within the primary nozzle system.

Thus, in this analogy, the basic mechanism responsible for thrust augmentation clearly may be identified as the improved transfer efficiency from the primary to the secondary because of the presence of the shroud which accelerates the secondary and decreases the velocity difference. However, the optimization of this process in the presence of various loss mechanisms is not straightforward because of the many parametric interactions involved.

Experiments Concerning Free-Fall Simulation

M. J. Houghton*
The University of Southampton, Southampton, England

A Vertical Wind Tunnel

THE aerodynamics and limitations of the human body in free fall is an interesting[1] and potentially important[2] area for research. A proposal has been made[2] concerning a vertical wind tunnel, specially designed to establish those conditions pertaining to free-fall parachuting, in which a student parachutist can develop his skills without danger of serious collision with the surrounding wind tunnel structure. The major advantages over conventional free-fall training are: a) safety, b) cheapness, c) time saving (e.g. weather independent operation), d) nonspecialist training and in evaluating free-fall stabilizing equipment (drogues, etc.) for inexperienced or heavily laden free fallers.

Here it is emphasized that this facility provides a very useful research tool allowing easy access to the air flow in a "nonhostile" laboratory environment; operation of the simulator for 1 hour is equivalent to 120 conventional descents from 7,000 ft. in terms of free-fall time.

The essential features of the simulator are: 1) a negative vertical velocity gradient – induced by the funnel shaped working section (axis a b is vertical); 2) a positive radial velocity gradient-induced by suitable ducts or windmills (not shown in Fig. 1a) inside the effuser. Features (1) and (2) imply that the equilibrium of the free faller ("Suspended" by the vertical airflow) is stable against induced vertical and horizontal displacements; a harness is essential for exercises, or studies, involving horizontal "tracking" – a strain gage measuring performance.

Stable equilibrium was indicated experimentally by the motion-free suspension of a free-falling shuttlecock (or table tennis ball etc.) within the center of the working section of Fig. 1b. Unfortunately the power requirement for a full scale

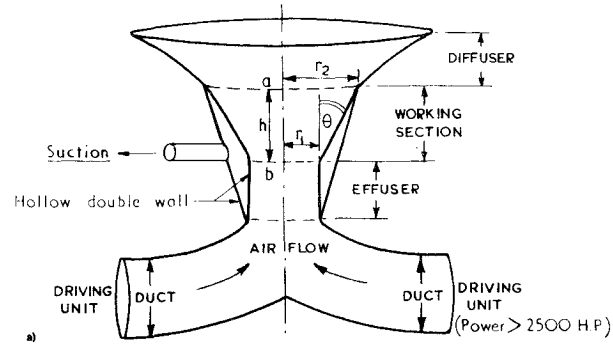

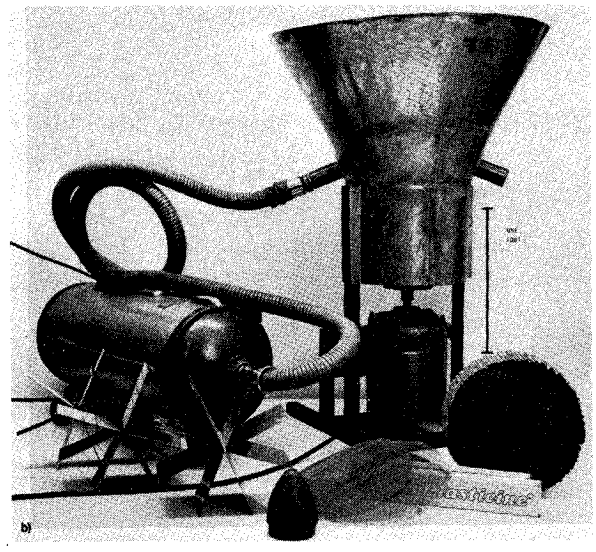

Fig. 1 Training aid or simulator (model b is identical to a apart from the single driving unit). a) Open circuit version, side view (internal vanes are not indicated). Suction through holes (not shown) in the inner working section wall prevents flow separation[3] which occurs if $\theta > 6°$. b) Working scale model. Vanes, honeycomb, etc. used in eliminating swirl and in shaping the flow velocity profile are shown in the foreground. Plasticine was used to shape the inner working section wall.

Received Oct. 5, 1976; revision received Dec. 7, 1976.
Index categories: Research Facilities and Instrumentation.
*Research Fellow, Space Physics Group, Dept. of Physics.

open circuit version (e.g. $r_1 = 10$ ft, $r_2 = 15$ ft, $h = 20$ ft) exceeds 5000 hp (even with a power factor[3] $\lambda \equiv [\frac{1}{2}\rho U^3 \pi r_1^2 / \text{input power}] \simeq 1$); the running cost ~ £300 ($510) per hour.

An Equivalent Vertical Water Tunnel

The drag force on a free faller is given by $F_D = [\frac{1}{2}\rho U^2 A] \times C_D$ (standard notation) where, at terminal velocity U, $F_D = w \cdot g$ (body weight). When immersed in water with doubled body weight ($2\ w \cdot g$) buoyancy forces are cancelled hence $U^{(\text{water})} = U^{(\text{air})} \sqrt{\rho^{(\text{air})}/\rho^{(\text{water})}}$ (assuming that the drag coefficient $C_D{}^{(\text{air})} = C_D{}^{(\text{water})}$). Thus if $U^{(\text{air})} = 176$ fps then $U^{(\text{water})} = 6.3$ fps. Fortuitously the kinematic viscosity of air is 1.6×10^{-4} ft^2/sec (and $\rho^{(\text{air})} = 0.08$ lb/ft^3) while that of (warm) water is 0.6×10^{-5} ft^2/sec. Thus almost perfect dynamical similarity is achieved. Further, the power requirement is about one thirtieth that of an equivalent wind tunnel with the same power factor λ (e.g. $5000/30 \simeq 170$ hp).

Conclusions

1) The proposed state of stable equilibrium has been demonstrated with a very crude working scale model (Fig. 1b) and the apparently unrealistic velocity profile [features (1) and (2)] is rather easy to achieve in practice.

2) Flow separation at the walls was quite easily prevented by suction.

3) Swirl was a major problem although it produced the previously stated requirement (2). Eliminating swirl with honeycomb or wide vanes (i.e. requiring a blade width $> r_1$, Fig. 1a) greatly reduced efficiency (i.e. $\lambda < 1$). Either 1) incorporating honeycomb while increasing efficiency with a return circuit[3], or 2) eliminating swirl by placing the fan downstream (i.e. above) the working section might prove too expensive.

4) A vertical water tunnel is vastly superior to the suspended harness for training purposes while also allowing for studies of dynamically similar flows at extremely low power consumption and cost.

References

[1] Sellick, B., *Skydiving*, 1st ed., Prentice Hall, N.Y., 1961.

[2] Houghton, M. J., "A Simulator for Training Free Fall Parachutists," submitted to U.K.A.E.A. Patents Office, London, July 1971.

[3] Pankhurst and Holder, *Wind Tunnel Technique*, 1st ed., Pitmans and Sons Ltd, London, 1952, pp. 62-65.

Mach 6 Flowfield Survey at the Engine Inlet of a Research Airplane

Charles B. Johnson* and Pierce L. Lawing*
NASA Langley Research Center, Hampton, Va.

Introduction

ONE early conceptual design for a new high-speed research airplane, which resulted from a joint USAF/NASA study, has been reported in Ref. 1. The vehicle is to be air launched from a B-52 and rocket boosted to Mach 6. An important research experiment is the testing of an airframe-integrated scramjet, which is mounted on the lower surface of the vehicle. During heat-transfer tests conducted on a 1/29-scale epoxy model of the configuration,[2] it was noted that there was a pronounced streak of low heating (cold streak) on the centerline of the bottom surface of the fuselage. It was speculated that the cold streak was caused by inflow on the forebody of the delta planform, and this inflow caused a thickening of the boundary layer along the centerline. Since one of the primary objectives of the research airplane would be the testing of an integrated airbreathing propulsion system, it was feared that the centerline cold streak and associated boundary-layer thickening on the centerline of the forebody would affect the performance of the scramjet engine. Therefore, flowfield surveys were conducted to better define the nature of the vehicle forebody flowfield at the inlet location of the scramjet engine. It is the purpose of this Note to present some results of the flowfield survey.

Received December 15, 1976.
Index categories: Boundary Layers and Convective Heat Transfer-Turbulent; Airbreathing Propulsion; Configuration Design.

*Aero-Space Technologist, Hypersonic Aerodynamics Branch, High-Speed Aerodynamics Division. Member AIAA.

Results and Discussion

Phase-change paint heat-transfer patterns on the bottom of the 1/29-scale epoxy model at four angles of attack are shown in Fig. 1. The configuration has a flat-bottom forebody extending to the scramjet engine inlet. The vertical sides of the scramjet engine are simulated in Fig. 1 by two engine side plates located just slightly downstream of the point at which the wing joins the fuselage. The scramjet inlet would be located at the plane joining the upstream ends of the two engine side plates. The phase-change pattern for $\alpha = 4°$ in Fig. 1 is the same data as shown for a similar view in Ref. 2. The cold streak along the centerline of the forebody exists for both $\alpha = 4°$ and $\alpha = 8°$. At $\alpha = 12°$ there is just a trace of the cold streak downstream of the unmelted paint located about one-third of the distance along the forebody. At $\alpha = 16°$, the cold streak on the centerline apparently has disappeared. The series of photographs in Fig. 1 indicates that the cold streak tends to weaken appreciably for increasing angles of attack between $\alpha = 8°$ and $\alpha = 12°$.

An oil flow photograph is shown in Fig. 2 at $\alpha = 4°$ and a Reynolds number of 15.5×10^6, based on freestream flow conditions and the body length, $L = 0.508$ m (20 in.). The

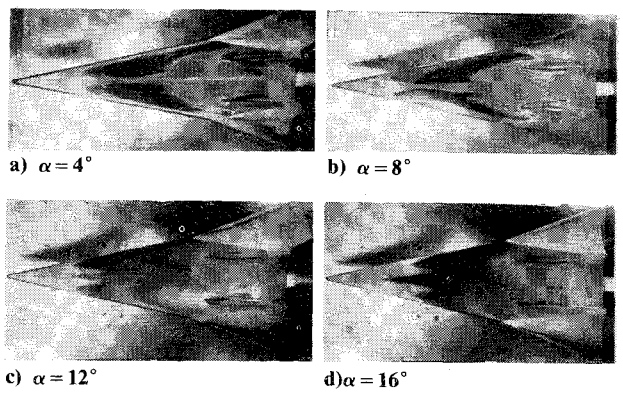

a) $\alpha = 4°$ b) $\alpha = 8°$

c) $\alpha = 12°$ d) $\alpha = 16°$

Fig. 1 Bottom view of phase-change heat-transfer patterns on the epoxy model at $R_{\infty,L} = 13 \times 10^6$ and Mach 6.

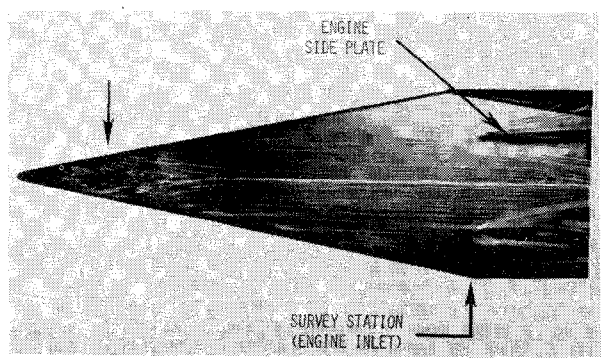

Fig. 2 Oil flow on the epoxy model forebody.